

Recent Developments in the Analysis of X-Ray Raman Scattering

J. A. Soininen*, J. J. Rehr†, A. Mattila*, S. Galambosi* and K. Hämäläinen*

* Division of X-ray Physics, Department of Physical Sciences, POB 64, FI-00014 University of Helsinki, Finland
† Department of Physics, University of Washington, Seattle, Washington 98195-1560, USA

Abstract. Non-resonant inelastic scattering of hard x-rays from core-electron excitations is often called x-ray Raman scattering (XRS). In the low momentum transfer limit, the XRS spectrum is proportional to the x-ray absorption coefficient. However, additional information is available when the magnitude of the momentum transfer is increased in XRS experiments. In this paper we will review recent developments in first-principles methods to analyze XRS spectra. Additionally, the importance of the momentum transfer dependent single-particle excitation matrix elements in the analysis will be discussed. We show how the momentum transfer dependence of the spectra can be used to extract information on the spatial symmetries of the final state electrons. We demonstrate this on experimental data for the Li K edge in Li metal.

Keywords: inelastic x-ray scattering, first principles methods

PACS: 78.70.Ck, 71.10.-w, 71.15.Qe,

Although non-resonant x-ray Raman scattering (XRS) can be considered a novel spectroscopy the first unambiguous experimental observations of it were done over four decades ago [1]. Due to the development of third generation x-ray sources the number of XRS applications in the study of materials has been steadily increasing, although XRS is not as routinely utilized as, for example, x-ray absorption spectroscopy (XAS). One of the motivations for doing XRS is the possibility of obtaining information similar to XAS for light elements but with hard x-rays. This close relationship between XAS and XRS at low momentum transfers was discussed already by Mizuno et al. [2]. The use of hard x-rays as a probe makes XRS a useful alternative, for example, in the case of difficult sample environments like high pressure, [3] or in the study of liquids [4]. Additionally, the use of hard x-rays means that in the XRS experiments, genuine bulk properties are always studied and method is not surface sensitive.

At low momentum transfers the XRS spectrum is dominated by dipole allowed transitions, giving the same information content as XAS experiments. Therefore, the standard analysis tools originally developed for XAS can be directly applied to XRS data. As the magnitude of the momentum transfer is increased, other non-dipole excitation channels gain weight. This was already discussed by Doniach et al. [5] using a simple model case. They pointed out that although the spectrum itself is a result of complex many body processes, the momentum transfer dependent matrix elements are essentially a single particle property. One of the reasons why the momentum transfer dependence of XRS is not widely used has been the lack of quantitative analysis tools specifically

designed for such experiments. In this work we describe some of the recent advances in the development of such tools.

In non-relativistic Born approximation the double differential cross section for NRIXS is given by [6, 7]

$$\frac{d^2\sigma}{d\Omega d\omega} = \left(\frac{d\sigma}{d\Omega} \right)_{Th} S(\mathbf{q}, \omega), \quad (1)$$

where $(d\sigma/d\Omega)_{Th}$ is the Thomson scattering cross-section depending on the scattering angle, and the properties of the incident and outgoing photons i.e. the photon polarisation vector and energy $\{\hat{\epsilon}_i, \omega_i\}$. The response of the sample to the scattering event is directly related to the dynamic structure factor $S(\mathbf{q}, \omega)$. The dynamic structure factor depends only on the momentum \mathbf{q} and energy ω transferred in the scattering process. In theory this means that, unlike in x-ray absorption, in NRIXS the incident energy can be chosen freely and only the energy difference $\omega = \omega_1 - \omega_2$ determines what kind of excitations are probed. However, in practice the experiments discussed in this work are typically accomplished with incident energies in the range of 8 keV to 14 keV and energy transfers of few hundreds of eV's. The momentum transfer is varied in the experiment to change the spectral weight of different types of excitations. When the energy transfer is close to the binding energy of a core state one can study the core-excited states i.e. XRS.

The dynamic structure factor can be expressed in terms of many-particle initial $|I\rangle$ and final $|F\rangle$ states as

$$S(\mathbf{q}, \omega) = \sum_F |\langle F | \sum_n e^{i\mathbf{q}\cdot\mathbf{r}_n} | I \rangle|^2 \delta(\omega + E_I - E_F), \quad (2)$$

where the sum n is over all the electrons in the system and the energies of the electrons states are given by E_I and

E_F . Assuming Slater determinant type initial states the excitation operator can be written in second quantized form as

$$\hat{\rho}_{\mathbf{q}}^{\dagger} = \sum_j^{\text{occ}} \sum_{i \neq j}^{\text{unocc}} \langle \phi_i | e^{i\mathbf{q} \cdot \mathbf{r}} | \phi_j \rangle \hat{a}_i^{\dagger} \hat{a}_j,$$

where it was additionally assumed that the energy transfer is finite. For core-excited states the occupied states are atomic-like tightly-bound states with well defined lm . In this case we expand the exponential in spherical Bessel functions j_l and spherical harmonics Y_{lm} as

$$\exp(i\mathbf{q} \cdot \mathbf{r}) = 4\pi \sum_{lm} i^l j_l(qr) Y_{lm}^*(\hat{\mathbf{q}}) Y_{lm}(\hat{\mathbf{r}}). \quad (3)$$

Thus we see that the weight of different angular momentum components of the final state ϕ_i is changed when the momentum transfer is changed. At the $q \rightarrow 0$ limit, assuming that the initial and final state are orthogonal, the dipole allowed transitions dominate the XRS spectrum

$$\lim_{q \rightarrow 0} \langle \phi_i | e^{i\mathbf{q} \cdot \mathbf{r}} | \phi_j \rangle = i \langle \phi_i | \mathbf{q} \cdot \mathbf{r} | \phi_j \rangle + O(q^2), \quad (4)$$

and, as mentioned earlier, one obtains similar information as in XAS. In XRS, however, the increase of the momentum transfer can be used to make the other terms $\propto q^2$ become dominant, and effectively to select the spatial symmetry of the final state.

A true quantitative analysis of XRS spectra has remained a challenge due to the difficulties in correctly describing the many-body effects in the core-excited states. One possible method for including these effects is the Bethe-Salpeter equation (BSE) approach [8]. This approach has been successfully applied to materials ranging from metals [8] to insulators [9] including the momentum transfer dependence. Indeed, the momentum transfer dependence of the XRS was used to experimentally identify a *s*-type exciton at the Fluorine K-edge in LiF [10]. The BSE method has also been used to analyze the momentum transfer dependence by decomposing the contributions from final state with given spatial symmetry (i.e. *s*, *p*, or *d*) [11, 12, 13]. However, The method of Ref. [8] is based on band structure calculations and is hard to apply to aperiodic systems. To have access to also aperiodic systems an extension of the FEFF8 [14] code to XRS was developed [15]. This method also opens up the possibility of analysing the momentum transfer dependence in the extended energy range in a similar way as is done for the extended x-ray absorption spectroscopy (EXAFS). Finally, a method was proposed in Ref. [15] for obtaining the different components of angular-momentum projected local density of states (IDOS) from the momentum transfer dependent XRS data. This approach was recently [16] used to obtain *s*-type and *p*-type core-excited state IDOS at the boron site in MgB₂ from XRS spectra [13].

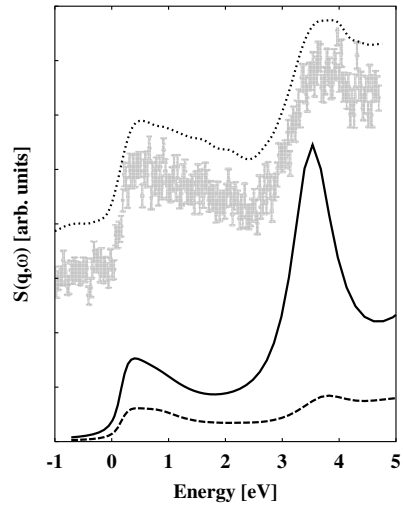


FIGURE 1. The experimental XRS data with errorbars for the K edge in Li metal is from the experiment reported in Ref. [18]. The calculated total spectrum is given by the solid line. The dipole allowed contribution to the calculated spectrum is also shown (dashed line). The smoothed experimental spectrum used in the final analysis is given by the dotted line. The raw and smoothed experimental data are shifted vertically for clarity.

The momentum transfer dependence of XRS spectra was studied already nearly two decades ago in Li with a moderate energy resolution [17]. More recently, the first few eV of the K-edge were measured with an energy resolution of 80 meV [18]. In this paper a small momentum transfer ($q_1 = 0.46$ a.u.) spectrum is compared to the *p*-type IDOS, and a large *q* spectrum ($q_2 = 5.15$ a.u.) to *s*-type IDOS. In Fig. 1 we show the experimental spectra for the large *q* case together with the calculated spectra. All the spectra were shifted so that the onset of the K-edge spectrum is at 0 eV. The calculations were done with the real-space multiple scattering method (RSMS) [15]. In addition to the calculated total spectrum, we also show the contribution from the dipole allowed (*p*-type final) transitions. This analysis shows that about a third of the spectrum comes from the dipole allowed transitions in this energy range. Clearly, this effect must be taken into account before comparison to the calculated IDOS.

In order to extract the experimental IDOS we use the method proposed in [15] and applied to MgB₂ in Ref. [16]. To do this, we use the fact that in RSMS, the XRS spectra for polycrystalline Li is linearly related to the IDOS components $\rho_l(E)$ [15]

$$S(q, \omega) = \sum_l (2l+1) |M_l(q, E)|^2 \rho_l(E), \quad (5)$$

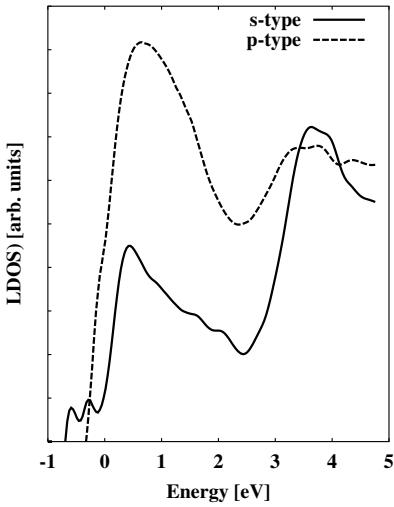


FIGURE 2. Local densities of states for Li site in Li metal. The *p*-type LDOS is given by the dashed line and *s*-type by the solid line.

where the matrix elements are

$$|M_l(q, E)|^2 = (2l_i + 1) \sum_{l'} (2l' + 1) \left| \begin{pmatrix} l_i & l' & l \\ 0 & 0 & 0 \end{pmatrix} \times \int r^2 dr R_l(r, E) j_{l'}(qr) R_i(r) \right|^2. \quad (6)$$

and E is the energy of the final state electron. In the matrix elements the radial part $R_i(r)$ ($R_l(r, E)$) of the initial (final) electron state has been used. Eq. 5 can be understood as linear equation relating the experimentally determined dynamic structure factor to the density of states, when matrix elements are known. To use this equation we first apply a smoothing spline to the experimental spectra both at the low and high momentum transfer limit (shown in Fig. 1 for the large momentum transfer). A constant background was subtracted from the experiment and we normalize the spectra using that calculated within the energy range available. The low momentum transfer spectrum is dominated by the dipole allowed transitions [19] and we can obtain the *p*-type LDOS as $\rho_1(E) = S(q_1, \omega)/(3M_1(q_1, E))$. This method is similar to that used by Ankudinov et al. in the analysis of XAS [20]. Next we can obtain dipole forbidden contribution to the high momentum transfer experiment simply by $S_{non-dip}(q_2, \omega) = S(q_2, \omega) - 3|M_1(q_2, E)|^2\rho_1(E)$ and from it, the *s*-type LDOS. We show the *s*-type and *p*-type densities of states obtained this way in Fig. 2. The resulting LDOS is in good agreement with the calculated LDOS in Ref. [18].

CONCLUSIONS

We have reviewed recent developments in the analysis of XRS spectra. The emphasis is on works where the analysis was carried out including both the direction and magnitude dependence of the momentum transfer in XRS. Novel information based on the momentum transfer dependence of XRS spectra was described. As an example, we re-analyzed the high resolution Li K-edge XRS experiment [18] obtaining the local angular momentum projected densities of states.

ACKNOWLEDGMENTS

This work was supported by the Academy of Finland (Contract No. 1201291/110571), and for JJR by the US Department of Energy (Grant DE-FG03-97ER45623), and was facilitated by the DOE Computational Materials Science Network.

REFERENCES

1. T. Suzuki, *J. Phys. Soc. Jpn.* **22**, 1139 (1967).
2. Y. Mizuno, and Y. Ohmura, *J. Phys. Soc. Jpn.* **22**, 445 (1967).
3. Y. Meng et al., *Nature Materials* **3**, 111 (2004).
4. Ph. Wernet et al., *Science* **304**, 995 (2004).
5. S. Doniach, P. M. Platzman, and J. T. Yue, *Phys. Rev. B* **4**, 3345 (1971).
6. W. Schülke, “Inelastic scattering by Electronic Excitations” in *Handbook of Synchrotron Radiation* vol 3., edited by G. S. Brown and D. E. Moncton, North-Holland, Amsterdam, 1991, pp. 565-637.
7. K. Hämäläinen and S. Manninen, *J. Phys.: Condens. Matt.* **13**, 7539 (2001).
8. J. A. Soininen, and E. L. Shirley, *Phys. Rev. B* **64**, 165112 (2001).
9. J. A. Soininen et al., *J. Phys.: Condens. Matt.* **13**, 8039 (2001).
10. K. Hämäläinen et al., *Phys. Rev. B* **65**, 155111 (2002).
11. C. Sternemann et al., *Phys. Rev. B* **68**, 035111 (2003).
12. C. Sternemann et al., *Phys. Rev. B* **72**, 035104 (2005).
13. A. Mattila et al., *Phys. Rev. Lett.* **94**, 247003 (2005).
14. A. L. Ankudinov, B. Ravel, J. J. Rehr, and S. D. Conradson, *Phys. Rev. B* **58**, 7565, (1998).
15. J. A. Soininen, A. L. Ankudinov, and J. J. Rehr, *Phys. Rev. B* **72**, 045136 (2005).
16. J. A. Soininen et al., *J. Phys.: Condens. Matt.* in print.
17. H. Nagasawa, S. Mourikis, and W. Schülke, *J. Phys. Soc. Jpn.* **58**, 710 (1989).
18. M. H. Krisch, F. Sette, C. Masciovecchio, and R. Verbeni, *Phys. Rev. Lett.* **78**, 2843 (1997).
19. The calculations indicated that only about 2% of the spectra comes from dipole forbidden transitions.
20. A. L. Ankudinov, A. I. Nesvizhskii, and J. J. Rehr, *J. Synchrotron Rad.* **8**, 92 (2001).